

Magnons and Magnetodielectric Effects in CoCr_2O_4 : Raman Scattering Studies

A. Sethi,^{1,*} T. Byrum,¹ R.D. McAuliffe,² S.L. Gleason,¹ J.E. Slimak,¹ D. P. Shoemaker,² and S. L. Cooper^{1,†}

¹*Department of Physics and Frederick Seitz Materials Research Laboratory,
University of Illinois, Urbana, Illinois 61801, USA*

²*Department of Materials Science and Engineering and
Frederick Seitz Materials Research Laboratory, University of Illinois, Urbana, Illinois 61801, USA*

Magnetolectric materials have generated wide technological and scientific interest because of the rich phenomena these materials exhibit, including the coexistence of magnetic and ferroelectric orders, magnetodielectric behavior, and exotic hybrid excitations such as electromagnons. The multiferroic spinel material, CoCr_2O_4 , is a particularly interesting example of a multiferroic material, because evidence for magnetolectric behavior in the ferrimagnetic phase seems to conflict with traditional noncollinear-spin-driven mechanisms for inducing a macroscopic polarization. This paper reports an inelastic light scattering study of the magnon and phonon spectrum of CoCr_2O_4 as simultaneous functions of temperature, pressure, and magnetic field. Below the Curie temperature ($T_C \sim 94$ K) of CoCr_2O_4 we observe a $\omega \sim 16 \text{ cm}^{-1}$ $\mathbf{q} = 0$ magnon having T_{1g} -symmetry, which has the transformation properties of an axial vector. The anomalously large Raman intensity of the T_{1g} -symmetry magnon is characteristic of materials with a large magneto-optical response and likely arises from large magnetic fluctuations that strongly modulate the dielectric response in CoCr_2O_4 . The Raman susceptibility of the T_{1g} -symmetry magnon exhibits a strong magnetic-field dependence that is consistent with the magnetodielectric response observed in CoCr_2O_4 , suggesting that magnetodielectric behavior in CoCr_2O_4 primarily arises from the field-dependent suppression of magnetic fluctuations that are strongly coupled to long-wavelength phonons. Increasing the magnetic anisotropy in CoCr_2O_4 with applied pressure decreases the magnetic field-dependence of the T_{1g} -symmetry magnon Raman susceptibility in CoCr_2O_4 , suggesting that strain can be used to control the magnetodielectric response in CoCr_2O_4 .

PACS numbers: 78.30.-j, 75.85.+t, 75.30.Ds, 75.47.Lx

I. INTRODUCTION

Multiferroics—materials exhibiting a coexistence of both magnetic and ferroelectric orders^{1,2}—have attracted substantial technological and scientific interest recently. The technological interest stems from the multifunctional properties exhibited by multiferroics, which make them potentially useful in device applications such as magneto-electric memories and switches. Multiferroics are scientifically interesting, in part, because they exhibit a variety of microscopic mechanisms that can result in an interesting interplay between ferroelectric and magnetic orders;² among other consequences, this interplay can spawn interesting dynamical properties in multiferroic materials, including electromagnons, i.e., hybrid excitations involving a coupling between optical phonons and spin waves via the magnetolectric interaction,^{3–14} and magnetodielectric effects.^{15–17}

Materials in which geometric frustration leads to non-collinear spin order and strong spin-lattice coupling are particularly rich material environments to find novel magnetolectric behavior.^{1,18} Transition-metal-oxide spinel materials (AB_2O_4), for example, exhibit both non-collinear spin orders and strong spin-lattice coupling that can lead to magnetolectric coupling, because the presence of magnetic ions on the B -site pyrochlore lattice of the spinel structure often leads to strong geometric frustration and consequent non-collinear orders that can generate multiferroic phenomena.² Magnetolectric effects are indeed realized

in some ACr_2O_4 spinels (*e.g.*, $A=\text{Co}^{2+}$ and Fe^{2+}), in which the competition among the various exchange interactions, J_{A-A} , J_{A-Cr} , and J_{Cr-Cr} , involving the A^{2+} ions and the Cr^{3+} $S = 3/2$ spins lead to complex magnetic orders.^{19,20}

CoCr_2O_4 , in particular, exhibits a succession of magnetic orders, including ferrimagnetic order below $T_C \sim 94$ K, incommensurate conical spiral order below $T_S \sim 26$ K, commensurate order below $T_L \sim 14$ K,^{21,22} as well as spin-driven multiferroic behavior and dielectric anomalies below T_S .^{23–25} Yet, the nature and origin of magnetolectric behavior in CoCr_2O_4 remains uncertain. Multiferroicity in CoCr_2O_4 has been associated with the spin-current mechanism²⁶ involving cycloidal spin order,²³ in which the induced electric polarization is generated by the non-collinear spins²⁷ via the inverse Dzyaloshinskii-Moriya interaction, $\mathbf{P} \sim \mathbf{e}_{ij} \times (\mathbf{S}_i \times \mathbf{S}_j)$. However, evidence for multiferroicity,^{17,20} structural distortion,¹⁷ and magnetodielectric behavior¹⁷ have also been reported above T_S in the ferrimagnetic state of CoCr_2O_4 , raising questions about the origin of multiferroic behavior in this material. Yang *et al.*, for example, have suggested that magnetodielectric behavior in CoCr_2O_4 results from the presence of multiferroic domains that are reoriented in the presence of a magnetic field.¹⁷ But magnetodielectric behavior in magnetic materials can also arise from magnetic fluctuations that induce shifts in optical phonon frequencies via strong spin-lattice coupling.¹⁶

Unfortunately, a lack of microscopic information regarding spin-lattice coupling has prevented a clear identi-

fication of the mechanism for magnetodielectric behavior in CoCr_2O_4 . The intersublattice exchange magnon has been observed in CoCr_2O_4 using infrared and terahertz spectroscopies^{28,29} and optical phonons in CoCr_2O_4 have been identified using Raman scattering^{30–32} and optical absorption²⁸ measurements. However, to our knowledge, there have been no microscopic studies of spin-lattice coupling in CoCr_2O_4 that could clarify the origin of magnetodielectric behavior in this material. The application of pressure^{33–35} would be a useful means of studying spin-lattice coupling and its role in magnetoelectric behavior in spinels such as CoCr_2O_4 ; indeed, *ab initio* calculations predict that pressure should enhance the macroscopic polarization in the multiferroic regime of CoCr_2O_4 .³² However, the effects of pressure on the magnetoelectric behavior and spin-lattice coupling in CoCr_2O_4 have not yet been experimentally investigated.

Raman scattering is a powerful tool for studying magnons,^{36,37} strong spin-lattice coupling^{36,38} and electromagnons^{39–42} in complex oxide materials. When used in conjunction with pressure and magnetic-field tuning, Raman scattering can provide pressure- and magnetic-field-dependent information about the energy and lifetime of phonons, magnons, and spin-phonon coupling effects. In this paper, we report an inelastic light (Raman) scattering study of magnon and phonon excitations in CoCr_2O_4 as simultaneous functions of temperature, pressure, and magnetic field. Below $T_C = 94$ K, we report the development in CoCr_2O_4 of a $\sim 16\text{ cm}^{-1}$ (2 meV) $\mathbf{q} = 0$ magnon excitation with T_{1g} symmetry. The anomalously large Raman scattering susceptibility associated with the T_{1g} symmetry magnon in CoCr_2O_4 is indicative of a large magneto-optical response arising from large magnetic fluctuations that couple strongly to the dielectric response; this coupling is likely associated with the dielectric anomalies²⁰ observed in the ferrimagnetic phase of CoCr_2O_4 . We also show that the Raman intensity of the T_{1g} -symmetry magnon in CoCr_2O_4 exhibits a strong suppression with increasing magnetic field, suggesting that the dramatic magneto-dielectric behavior^{17,43} observed in CoCr_2O_4 results from the magnetic-field-induced suppression of magnetic fluctuations that are strongly coupled to phonons.¹⁶ Using applied pressure to increase the magnetic anisotropy in CoCr_2O_4 results in a decreased magnetic field-dependence of the T_{1g} -symmetry magnon Raman intensity in CoCr_2O_4 , suggesting that pressure or epitaxial strain can be used to control magnetodielectric behavior and the magneto-optical response in CoCr_2O_4 by suppressing magnetic fluctuations.

II. EXPERIMENTAL METHODS

A. Crystal Growth and Characterization

CoCr_2O_4 crystals were grown by chemical vapor transport (CVT) following a procedure described by Ohgushi

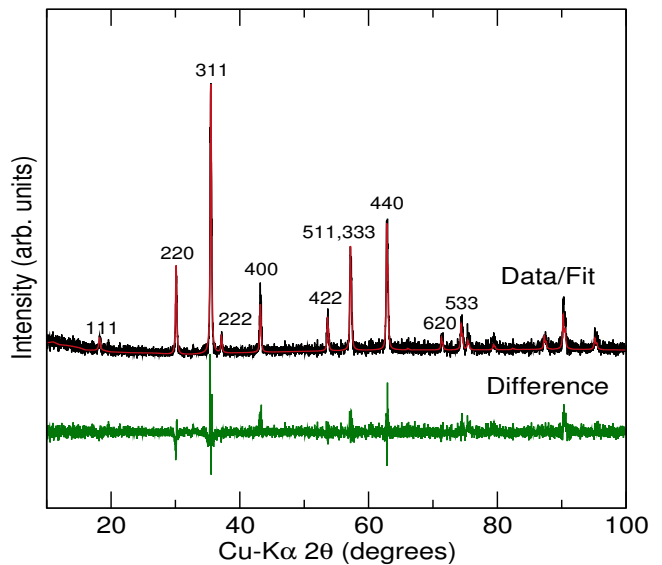


FIG. 1: X-ray diffraction pattern and Rietveld fit of CoCr_2O_4 at 298 K. The Miller indices for a cubic unit cell with cell parameter $a = 8.334(1)\text{Å}$ are also shown.

et al.⁴⁴ Polycrystalline powder samples of CoCr_2O_4 were first synthesized using cobalt nitrate hexahydrate (Strem Chemicals 99%) and chromium nitrate nonahydrate (Acros 99%). The nitrates were combined in stoichiometric amounts and dissolved in water. The solution was heated to 350°C and stirred using a magnetic stir bar at 300 rpm until all of the liquid evaporated. The remaining powder was heated in an alumina crucible at 900°C for 16 hours and then air quenched. Crystal samples of CoCr_2O_4 were grown by CVT using CrCl_3 as a transport agent. 2.0 g of polycrystalline samples and 0.04 g of CrCl_3 were sealed in an evacuated quartz ampoule, which was placed inside a three-zone furnace having 950°C at the center with a temperature gradient of $10^\circ\text{C}/\text{cm}$ for one month. Crystals with typical dimensions of $2 \times 2 \times 2\text{ mm}^3$ were obtained.

The CoCr_2O_4 crystals were characterised using x-ray diffraction and magnetization measurements. Crystals of CoCr_2O_4 were ground to a powder to obtain the x-ray diffraction pattern using a Siemens-Bruker D5000 diffractometer using $\text{Cu-K}\alpha$ radiation shown in Fig. 1. Rietveld refinement of the CoCr_2O_4 cell to the XRD data was performed using XND Rietveld,⁴⁵ and indicates a pure sample with $Fd\bar{3}m$ symmetry and a lattice constant of $8.334(1)\text{Å}$, which agrees with the established structure.²⁸ The $\langle 110 \rangle$ reflections from a single crystal of CoCr_2O_4 were measured, and no evidence of twinning imperfections was found. The field-cooled dc magnetization data on the CoCr_2O_4 powder from which our crystal sample was obtained was collected using a Quantum Design MPMS-3 and is shown as a function of temperature in Fig. 2. Our results are similar to existing data.²⁴ In particular, the sudden increase in the molar susceptibility, χ_m at $T \sim 94$ K marks the onset of ferrimagnetic

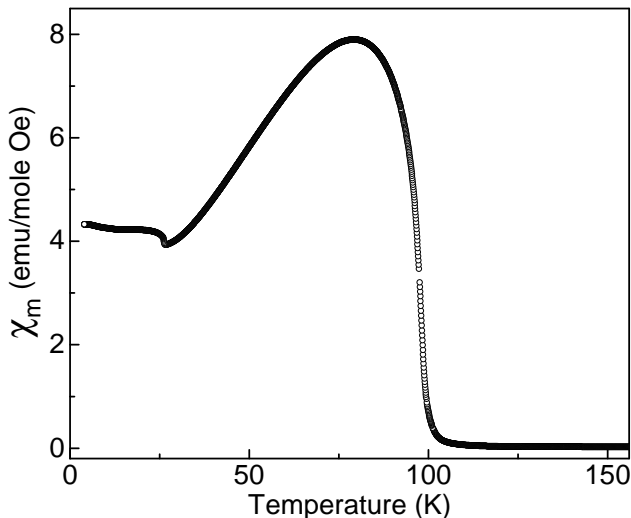


FIG. 2: Molar susceptibility of CoCr_2O_4 as a function of temperature measured in an applied field of 100 Oe.

ordering. The change in slope of the graph at $T \sim 26$ K and an additional small anomaly at $T \sim 14$ K correspond to the incommensurate and commensurate spiral ordering, respectively, in CoCr_2O_4 .

B. Raman Scattering Measurements

Raman scattering measurements were performed using the 647.1 nm excitation line from a Kr^+ laser. The incident laser power was limited to 5 – 10 mW, and was focused to a ~ 50 μm -diameter spot to minimize laser heating of the sample. Sample heating by the laser was estimated to be in the range 5 – 7 K, and this estimated laser heating is included in the temperatures given in the results section. The scattered light from the samples was collected in a backscattering geometry, dispersed through a triple stage spectrometer, and then detected with a liquid-nitrogen-cooled CCD detector. The samples were inserted into a continuous He-flow cryostat, which was horizontally mounted in the open bore of a superconducting magnet.⁴⁶ This experimental arrangement allows Raman scattering measurements under the simultaneous conditions of low temperature (3 – 300 K), high magnetic fields (0 – 9 T), and high pressures (0 – 100 kbar). To determine the symmetries of the measured Raman excitations in zero magnetic field, linearly polarized incident and scattered light were used for various crystallographic orientations of the sample. In the magnetic field measurements, circularly polarized light was used to avoid Faraday rotation of the light polarization.

Magnetic field measurements were performed in both Voigt ($\mathbf{k} \perp \mathbf{M} \parallel \mathbf{H}$) and Faraday ($\mathbf{k} \parallel \mathbf{M} \parallel \mathbf{H}$) geometries, where \mathbf{k} is the wavevector of the incident light and \mathbf{M} is the magnetization direction.⁴⁶ Because of the very small anisotropy field in CoCr_2O_4 ($H_A \leq 0.1$ T),²⁹ the

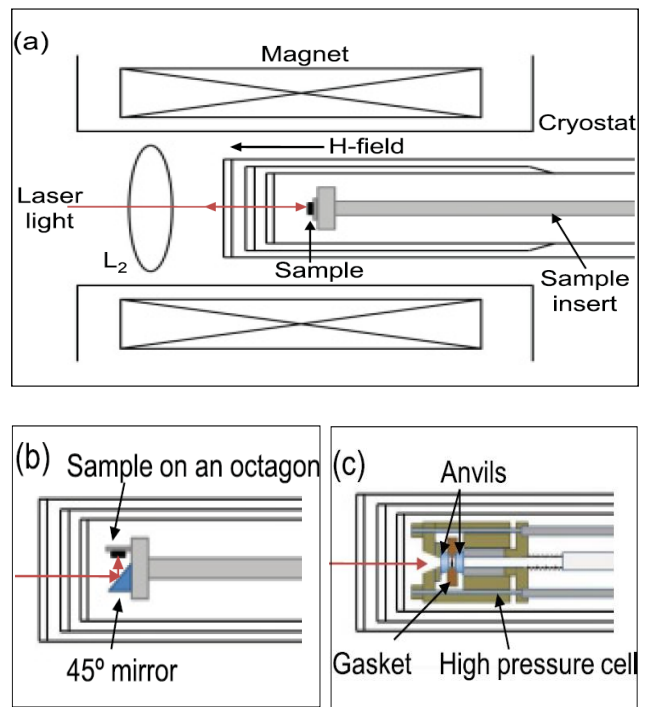


FIG. 3: Illustrations showing the experimental arrangements used for different high-magnetic-field and high temperature Raman scattering experiments at low temperatures in this study.⁴⁶ (a) Configuration for high-magnetic field measurements in the Faraday ($\mathbf{k} \parallel \mathbf{H}$) geometry, where \mathbf{k} is the wavevector of the incident light and \mathbf{H} is the applied magnetic field direction. (b) Configuration for high-magnetic-field measurements in the Voigt ($\mathbf{k} \perp \mathbf{H}$) geometry. (c) Configuration for high pressure measurements using a diamond anvil cell.

net magnetization \mathbf{M} was assumed to follow the applied field \mathbf{H} in all experiments performed. To verify this, we confirmed that the field-dependence of the Raman spectrum was independent of the crystallographic orientation of the applied field. The field measurements in the Faraday geometry were performed by mounting the sample at the end of the insert, as illustrated in Fig. 3(a), so that the wavevector of the incident light is parallel to the applied field. The Voigt geometry was achieved by mounting the sample on an octagon plate, which was mounted sideways on the sample rod, as illustrated in Fig. 3(b). The incident light was guided to the sample surface with a 45° mirror mounted on the sample rod. This sample mounting arrangement allows the magnetic field to be applied perpendicular to the wavevector of the incident light, $\mathbf{k} \perp \mathbf{M} \parallel \mathbf{H}$.

High pressure measurements were performed using a miniature cryogenic diamond anvil cell (MCDAC) to exert pressure on the sample via an argon liquid medium. The high-pressure cell was inserted into the cryostat as illustrated in Fig. 3(c), allowing the pressure to be changed *in situ* at low temperatures without any extra warm-

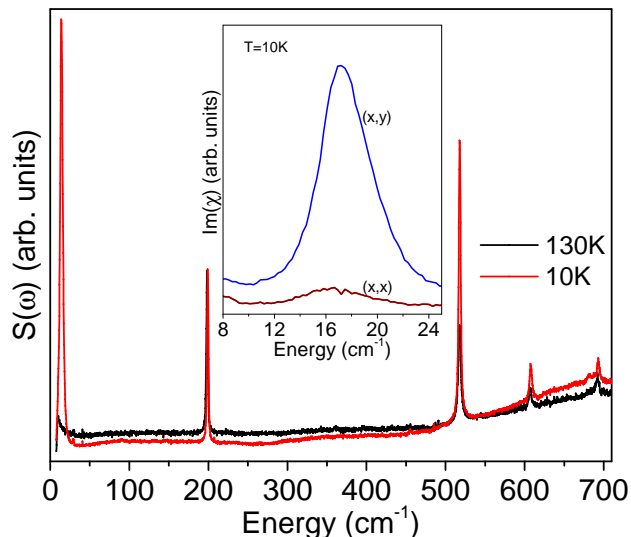


FIG. 4: Temperature-dependence of the Raman scattering intensity, $S(\omega)$, for CoCr_2O_4 at 10 K and 130 K, showing the phonon modes above 150 cm^{-1} and the T_{1g} symmetry magnon near 16 cm^{-1} that evolves for $T < 90 \text{ K}$. Inset shows the polarization dependence of the magnon in CoCr_2O_4 ; the presence of this mode only in the depolarized geometry for all crystallographic orientations is indicative of the T_{1g} symmetry, which transforms like an axial vector.

ing/cooling procedure. This arrangement also allows simultaneous high-pressure and high-magnetic field measurements in the Faraday ($\mathbf{k} \parallel \mathbf{M} \parallel \mathbf{H}$) geometry, as illustrated in Fig. 3(c).⁴⁶ The pressure was determined from the shift in the fluorescence line of a ruby chip loaded in the cell along with the sample piece.

III. TEMPERATURE DEPENDENCE OF THE MAGNETIC EXCITATION AT $P=0$ AND $B=0$

A. Results

Fig. 4 shows the $T = 10 \text{ K}$ and $T = 130 \text{ K}$ Raman spectra of CoCr_2O_4 between $0\text{-}700 \text{ cm}^{-1}$ in a scattering geometry with circularly polarized incident light and un-analyzed scattered light. The $T = 10 \text{ K}$ spectrum exhibits the five Raman-active phonon modes expected and previously observed^{30–32} for CoCr_2O_4 , including phonon modes at 199 cm^{-1} , 454 cm^{-1} , 518 cm^{-1} , 609 cm^{-1} , and 692 cm^{-1} (at $T = 10 \text{ K}$). In addition to the phonon modes, the $T = 10 \text{ K}$ spectrum in Fig. 4 has an additional mode that develops near 16 cm^{-1} ($\sim 2 \text{ meV}$) below $T = 90 \text{ K}$. The inset of Fig. 4 shows that the 16 cm^{-1} mode intensity is present only in the “depolarized” scattering geometry, *i.e.*, only when the incident and scattered light polarizations are perpendicular to one another, independent of the crystallographic orientation. This polarization dependence indicates that the

16 cm^{-1} mode symmetry transforms like the fully anti-symmetric representation, T_{1g} , which has the symmetry properties of an axial vector, characteristic of a magnetic excitation.^{47,48} Consequently, we identify the 16 cm^{-1} excitation as a $\mathbf{q} = 0$ T_{1g} symmetry magnon in CoCr_2O_4 . This interpretation is supported by the temperature-dependence of the 16 cm^{-1} T_{1g} -symmetry mode Raman scattering susceptibility, $\text{Im} \chi(\omega)$ (see Fig. 5(a)), where $\text{Im} \chi(\omega) = S(\mathbf{q} = 0, \omega)/[1 + n(\omega, T)]$, $S(\mathbf{q} = 0, \omega)$ is the measured Raman scattering response, and $[1 + n(\omega, T)]$ is the Bose thermal factor with $n(\omega, T) = [e^{\hbar\omega/k_B T} - 1]^{-1}$. Fig. 5(b) shows that the $\sim 16 \text{ cm}^{-1}$ T_{1g} symmetry mode energy (solid squares) decreases in energy (“softens”) with increasing temperature toward T_C —consistent with the temperature-dependence of the Co^{2+} sublattice magnetization²⁹—indicative of a single-magnon excitation.⁴⁷ Fig. 5(b) also shows that the amplitude of the Raman susceptibility, $\text{Im} \chi(\omega)$, associated with the 16 cm^{-1} T_{1g} -symmetry magnon mode (solid circles) is relatively insensitive to temperature and is comparable to that of the 199 cm^{-1} T_{2g} phonon. Notably, the 16 cm^{-1} T_{1g} symmetry magnon we observe in CoCr_2O_4 has a similar energy and temperature dependence to that of the exchange magnon observed previously in terahertz²⁸ and infrared spectroscopy²⁹ measurements of CoCr_2O_4 . Nevertheless, it is unlikely that the 16 cm^{-1} T_{1g} symmetry magnon we observe in CoCr_2O_4 is the same as the intersublattice exchange mode reported in infrared measurements, because T_{1g} is not an infrared-active symmetry. Note in this regard that the spinel structure of CoCr_2O_4 is expected to exhibit six $\mathbf{q} = 0$ magnon modes with 5 closely spaced optical branches,^{28,49–51} so we are likely observing a different optical magnon that is close in energy to that observed in infrared measurements.^{28,29}

B. Discussion and Analysis

The finite $\mathbf{q} = 0$ energy of the $\omega \sim 16 \text{ cm}^{-1}$ (2 meV) T_{1g} -symmetry magnon in CoCr_2O_4 primarily reflects the finite exchange, H_E , and anisotropy, H_A , fields in CoCr_2O_4 , according to $\omega = \gamma(2H_A H_E + H_A^2)^{1/2}$, where γ is the gyromagnetic ratio $g\mu_B/\hbar$.⁴⁸ Fig. 5 also shows that the 16 cm^{-1} T_{1g} symmetry magnon in CoCr_2O_4 is apparent to temperatures as high as $T \sim 60 \text{ K}$, indicating that the T_{1g} symmetry magnon in CoCr_2O_4 is dominated by the Co^{2+} sublattice spins, which order at a significantly higher temperature (94 K) than the Cr^{3+} sublattice (49 K).²⁹

Importantly, the Raman susceptibility of the 16 cm^{-1} T_{1g} symmetry magnon at $T=10 \text{ K}$ (for $H = 0 \text{ T}$ and $P = 0 \text{ kbar}$) (see Fig. 5) reflects the degree to which this magnon modulates the dielectric response, $\epsilon = 4\pi\chi_E$ (where χ_E is the electric susceptibility).^{52,53} Consequently, while Raman scattering from magnons is generally much weaker than Raman scattering from phonons,⁴⁷ Figs. 4 and 5 show that Raman intensity of

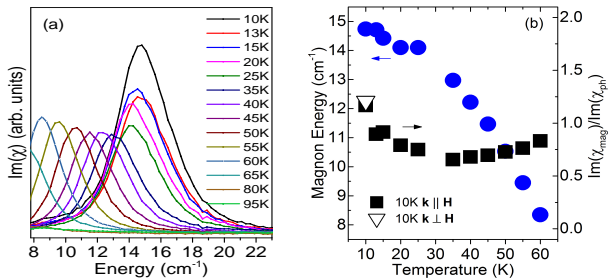


FIG. 5: (a) Raman scattering susceptibility, $\text{Im} \chi(\omega)$, of the T_{1g} -symmetry magnon of CoCr_2O_4 as a function of temperature. (b) Summary of the temperature dependence of the T_{1g} symmetry magnon energy (filled squares). Also shown in filled circles is a summary of the temperature dependence of the T_{1g} symmetry magnon Raman susceptibility amplitude normalized to the susceptibility amplitude of the 199 cm^{-1} T_{2g} optical phonon, $\text{Im} \chi_{\text{mag}}(\omega)/\text{Im} \chi_{\text{ph}}(\omega)$.

the T_{1g} -symmetry magnon is comparable to that of the Raman-active phonons in CoCr_2O_4 , indicative of a strong influence of this magnon on the dielectric response of CoCr_2O_4 .

The large Raman susceptibility of the T_{1g} symmetry magnon reflects a large magneto-optical response in CoCr_2O_4 , and is likely associated with strong magnetic fluctuations that modulate the dielectric response via strong spin-lattice coupling.^{52,54,55} Such large magnetic fluctuations are attributable to the weak anisotropy field in CoCr_2O_4 , $H_A \leq 0.1 \text{ T}$,²⁹ and can contribute in several ways to fluctuations in the dielectric response:^{52,54,55}

$$\delta\epsilon(m, l) = i f \delta m + g(\delta l)^2 + a(\delta m)^2 \quad (1)$$

where $\delta\epsilon$ is the dielectric response fluctuation, δm represents longitudinal fluctuations in the magnetization, δl represents fluctuations of the antiferromagnetic vector, and a , f , and g are constants. The first term in Eq. (1) is associated with the linear magneto-optical Faraday effect, the second term is associated with linear magnetic birefringence, and the final term is an isotropic “exchange” mechanism for magnon scattering that is present in non-collinear antiferromagnets.^{52,56} In non-collinear antiferromagnetic and ferrimagnetic materials with weak anisotropy—such as CoCr_2O_4 —strong single-magnon scattering can result from large fluctuations of both l and m . In particular, the one-magnon Raman scattering intensity, S , associated with large magnetic fluctuations of the antiferromagnetic vector at $H = 0$ is limited only by the anisotropy field, H_A (i.e., $S \propto 1/H_A$),⁵² which is very small in CoCr_2O_4 , $H_A \leq 0.1 \text{ T}$.²⁹

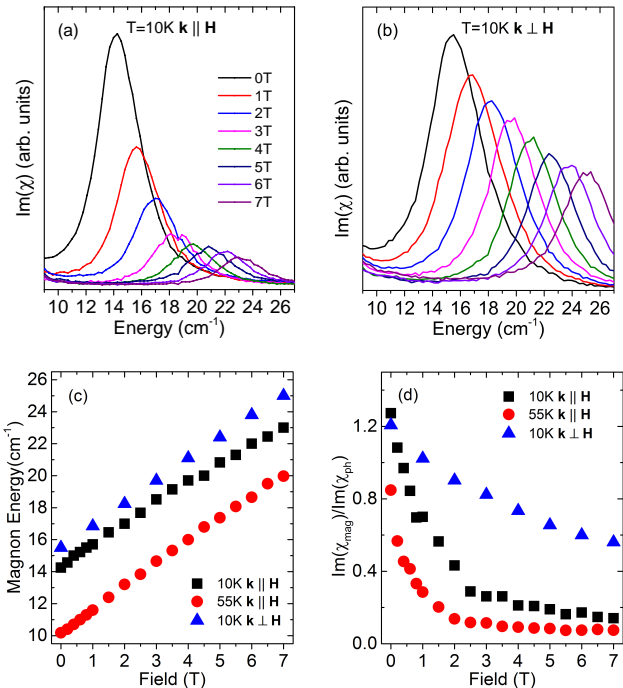


FIG. 6: Magnetic-field-dependence of the Raman scattering susceptibility, $\text{Im} \chi(\omega)$, of the T_{1g} -symmetry magnon in CoCr_2O_4 at $T = 10 \text{ K}$ in the (a) Faraday geometry ($\mathbf{k} \parallel \mathbf{M} \parallel \mathbf{H}$) and the (b) Voigt geometry ($\mathbf{k} \perp \mathbf{M} \parallel \mathbf{H}$). (c) Summary of the field dependences of the T_{1g} -symmetry magnon energy of CoCr_2O_4 at (filled squares) $T = 10 \text{ K}$ and (filled circles) $T = 55 \text{ K}$ in the Faraday geometry and at (filled triangles) $T = 10 \text{ K}$ in the Voigt geometry. (d) Summary of the field dependences of the amplitude of the T_{1g} -symmetry magnon Raman susceptibility normalized to the amplitude of the 199 cm^{-1} T_{2g} phonon Raman susceptibility at (filled squares) $T = 10 \text{ K}$ and (filled circles) $T = 55 \text{ K}$ in the Faraday geometry and at (filled triangles) $T = 10 \text{ K}$ in the Voigt geometry.

IV. MAGNETIC-FIELD-DEPENDENCE OF THE T_{1g} -SYMMETRY MAGNON IN CoCr_2O_4

A. Results

Fig. 6 shows the magnetic-field-dependence of the Raman susceptibility, $\text{Im} \chi(\omega)$, for the T_{1g} -symmetry magnon of CoCr_2O_4 at $P = 0 \text{ kbar}$ and $T = 10 \text{ K}$ with an applied magnetic field in both the (Fig. 6(a)) Faraday ($\mathbf{k} \parallel \mathbf{M} \parallel \mathbf{H}$) and (Fig. 6(b)) Voigt ($\mathbf{k} \perp \mathbf{M} \parallel \mathbf{H}$) geometries. Fig. 6(c) summarizes the field-dependences of the T_{1g} -symmetry magnon energy at both $T = 10 \text{ K}$ and $T = 55 \text{ K}$, showing that the T_{1g} -symmetry magnon energy exhibits a linear increase with increasing field. The shift in the T_{1g} -symmetry magnon energy with field, $d\omega/dH \sim 1.1 \text{ cm}^{-1}/\text{T}$ corresponds to a dimensionless ratio $\hbar\omega/\mu_B H = 2.4$. This ratio is close to the $T = 4$

K value of $\hbar\omega/\mu_B H = 2.5$ measured for the exchange magnon in CoCr_2O_4 ²⁹ and is consistent with the gyromagnetic ratio of 2.2 for Co^{2+} .^{28,57} Fig. 6(d) compares the field-dependence of the normalized T_{1g} -symmetry magnon intensity, $\text{Im} \chi_{mag}(\omega)/\text{Im} \chi_{ph}(\omega)$, in both the (filled circle and square) Faraday ($\mathbf{k} \parallel \mathbf{M} \parallel \mathbf{H}$) and (filled triangle) Voigt ($\mathbf{k} \perp \mathbf{M} \parallel \mathbf{H}$) geometries, where $\text{Im} \chi_{mag}(\omega)$ and $\text{Im} \chi_{ph}(\omega)$ are the Raman susceptibilities of the T_{1g} -symmetry magnon and 199 cm^{-1} T_{2g} phonon, respectively. Fig. 6(d) shows that there is a substantial decrease in the normalized T_{1g} -symmetry magnon intensity of CoCr_2O_4 with increasing field in both the Faraday ($\mathbf{k} \parallel \mathbf{M} \parallel \mathbf{H}$) and Voigt ($\mathbf{k} \perp \mathbf{M} \parallel \mathbf{H}$) geometries at $T = 10 \text{ K}$ and $T = 55 \text{ K}$. Note that the field-dependent decrease we observe in the T_{1g} -symmetry magnon intensity—which is particularly dramatic in the Faraday geometry ($\mathbf{k} \parallel \mathbf{M} \parallel \mathbf{H}$)—cannot be attributed to field-dependent changes in polarization or crystallographic orientation: the use of circularly polarized incident light in these experiments precludes field-dependent rotation of the incident polarization; and T_{1g} -symmetry modes appear in the depolarized scattering geometry independent of the crystallographic orientation of the sample.

B. Discussion and Analysis

The anomalously large decrease in the 16 cm^{-1} T_{1g} -magnon Raman intensity with increasing field in the Faraday geometry ($\mathbf{k} \parallel \mathbf{M} \parallel \mathbf{H}$) of CoCr_2O_4 (see Fig. 6) is quite different than the field-independent magnon Raman intensities observed in other spinel materials, such as Mn_3O_4 and MnV_2O_4 .³⁶ To clarify the anomalously strong field-dependence of the T_{1g} -symmetry magnon Raman intensity in CoCr_2O_4 , note that the magnon Raman intensity in the Faraday geometry is expected to be dominated by the linear magnetic birefringence contribution to dielectric fluctuations, $\delta\epsilon = g(\delta l)^2$.^{52,55,56} Thus, the strong decrease in the T_{1g} -symmetry magnon Raman intensity in the Faraday geometry likely reflects a field-induced decrease in fluctuations of the antiferromagnetic vector, δl . A similar field-dependent decrease in the single-magnon inelastic light scattering response associated with fluctuations of the antiferromagnetic vector was also observed in the canted antiferromagnet EuTe .⁵²

Fig. 6(b), 6(d) shows that there is a similar, albeit less dramatic, field-dependent decrease in the T_{1g} -symmetry magnon Raman intensity measured in the Voigt ($\mathbf{k} \perp \mathbf{M} \parallel \mathbf{H}$) geometry. This geometry is primarily sensitive to the Faraday ($\delta\epsilon = i f \delta m$) and isotropic exchange ($\delta\epsilon = a(\delta m)^2$) contributions to dielectric fluctuations, which are dominated by longitudinal fluctuations in the magnetization.^{52,55,56} Altogether, the suppression of the T_{1g} -symmetry magnon Raman scattering intensities in both Faraday and Voigt geometries is indicative of a field-induced suppression of both transverse and longitudinal magnetic fluctuations in CoCr_2O_4 .

The field-dependent suppression of the T_{1g} -symmetry

magnon Raman intensity in CoCr_2O_4 points to a specific microscopic mechanism for the magnetodielectric response observed in CoCr_2O_4 .^{17,20,43} Lawes *et al.* have pointed out that the field-induced suppression of magnetic fluctuations can contribute to the magnetodielectric response of a material via the coupling of magnetic fluctuations to optical phonons.¹⁶ This spin-phonon coupling contributes to the magnetodielectric response of a material through field-induced changes to the net magnetization.^{15–17,58} A simple phenomenological description for how the magnetization of a magnetoelectric material influences the dielectric response of the material is obtained by considering the free energy, F , in a magnetoelectric material with a coupling between the magnetization \mathbf{M} and polarization \mathbf{P} .^{15,17,58}

$$F(M, P) = F_0 + aP^2 + bP^4 - PE + cM^2 + dM^4 - MH + eM^2P^2, \quad (2)$$

where F_0 , a , b , c , d , and e are temperature-dependent constants, and M , P , E , and H are the magnitudes of the magnetization, polarization, applied electric field, and applied magnetic field, respectively. The dependence of the dielectric response on magnetization in a magnetoelectric material, $\epsilon(M)$, can be obtained from the second derivative of the free energy with respect to polarization P .^{15,17,58}

$$[\epsilon(M)]^{-1} \sim (\partial^2 F / \partial P^2) = 2a + 12bP^2 + 2eM^2, \quad (3)$$

which, for a negligible macroscopic polarization P in the material, can be written:^{15,17}

$$\epsilon(M) = 1/[2a + 2eM^2]. \quad (4)$$

Thus, the dielectric response, $\epsilon = 4\pi\chi_E$, decreases with increasing squared magnetization, M^2 and decreasing magnetic fluctuations.¹⁶

The above results suggest that both the magnetic-field-dependent decrease in the intensity of the 16 cm^{-1} T_{1g} -symmetry magnon (see Fig. 6) and the magnetodielectric response, $\Delta\epsilon(H)/\epsilon(0) = [\epsilon(H) - \epsilon(0)]/\epsilon(0)$, in CoCr_2O_4 ^{17,43} reflect magnetic-field-induced changes to magnetic fluctuations—particularly fluctuations associated with the antiferromagnetic vector—that are strongly coupled to phonons¹⁶ via the biquadratic contribution to the free energy, M^2P^2 (see Eq. (2)).

V. PRESSURE DEPENDENCE OF THE T_{1g} -SYMMETRY MAGNON IN CoCr_2O_4

A. Results

As discussed above, the strong T_{1g} -symmetry magnon Raman intensity of CoCr_2O_4 is believed to reflect

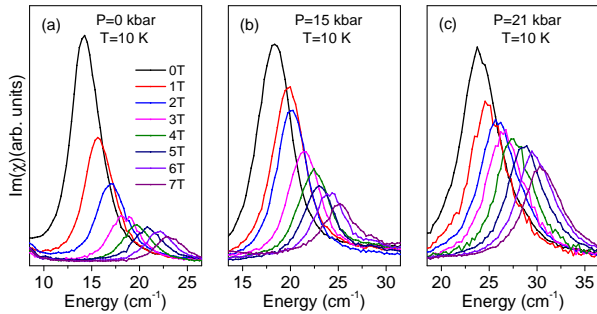


FIG. 7: Field-dependence in the Faraday ($\mathbf{k} \parallel \mathbf{M} \parallel \mathbf{H}$) geometry of the T_{1g} -symmetry magnon Raman susceptibility of CoCr_2O_4 at $T = 10$ K and at various applied pressures, including (a) $P = 0$ kbar, (b) $P = 15$ kbar, and (c) $P = 21$ kbar.

strong magnetic fluctuations that are coupled to long-wavelength phonons, which should also be associated with significant magneto-optical responses (both linear Faraday and linear magnetic birefringence) in CoCr_2O_4 . Our results show that the application of a magnetic field suppresses these fluctuations, leading to the substantial magnetodielectric response observed in CoCr_2O_4 . An alternative approach to suppressing magnetic fluctuations is to use applied pressure or strain to increase the crystalline anisotropy of CoCr_2O_4 . To investigate this possibility, magnetic-field-dependent measurements of the T_{1g} -symmetry magnon in CoCr_2O_4 were performed for different applied pressures.

Fig. 7 shows the field-dependence of the T_{1g} -symmetry magnon spectrum of CoCr_2O_4 in the Faraday ($\mathbf{k} \parallel \mathbf{M} \parallel \mathbf{H}$) geometry for different applied pressures at $T = 10$ K. Fig. 8(a) summarizes the field dependence of the T_{1g} -symmetry magnon energy at $T = 10$ K for different applied pressures, and Fig. 8(b) shows the amplitude of the T_{1g} -symmetry magnon Raman susceptibility (normalized by the amplitude of the 199 cm^{-1} T_{2g} phonon susceptibility) at $T = 10$ K for different applied pressures. The inset of Fig. 8(b) summarizes the pressure-dependence of the T_{1g} -symmetry magnon energy of CoCr_2O_4 for $H = 0$ T and $T = 10$ K.

B. Discussion and Analysis

The inset of Fig. 8(b) shows that the T_{1g} -symmetry magnon energy increases linearly with applied pressure at a rate of $d\omega/dP = 0.46\text{ cm}^{-1}/\text{kbar}$. This increase likely reflects a systematic increase in the anisotropy field, H_A , with increasing pressure, according to the relationship $\omega \sim (2H_A H_E)^{1/2}$. Additionally, the magnetic field dependence of the Raman spectrum of CoCr_2O_4 at different fixed pressures summarized in Fig. 8(a) shows that the field-dependent slope associated with the T_{1g} -symmetry magnon frequency, $d\omega/dH$, is insensitive to applied pres-

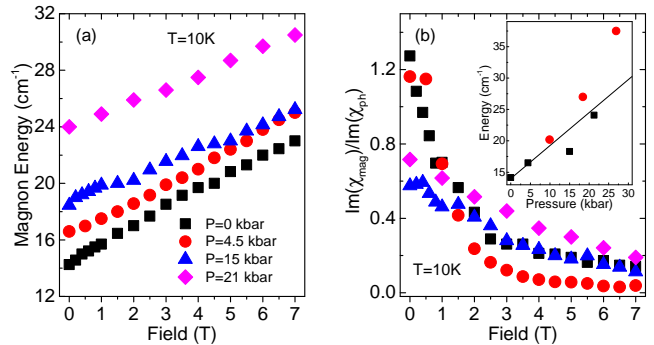


FIG. 8: (a) Summary of the field dependences in the Faraday ($\mathbf{k} \parallel \mathbf{M} \parallel \mathbf{H}$) geometry of the T_{1g} -symmetry magnon energy of CoCr_2O_4 at (filled squares) $T = 10$ K and at various pressures, including (filled squares) $P = 0$ kbar, (filled circles) $P = 4.5$ kbar, (filled triangles) $P = 15$ kbar, and (filled diamonds) $P = 21$ kbar. (b) Summary of the field dependences of the amplitude of the T_{1g} -symmetry magnon Raman susceptibility normalized to the amplitude of the 199 cm^{-1} T_{2g} phonon Raman susceptibility at $T = 10$ K and various pressures, including (filled squares) $P = 0$ kbar, (filled circles) $P = 4.5$ kbar, (filled triangles) $P = 15$ kbar, and (filled diamonds) $P = 21$ kbar. ((b) inset) Summary of the pressure-dependence of the T_{1g} -symmetry magnon energy in CoCr_2O_4 at $T = 10$ K and $H = 0$ T.

sure up to roughly 21 kbar, indicating that the gyromagnetic ratio associated with Co^{2+} is not strongly affected by these pressures in CoCr_2O_4 .

On the other hand, Figs. 7 and 8 also show that $H = 0$ T_{1g} -symmetry magnon Raman intensity, $\text{Im}\chi(\omega)$, systematically decreases relative to the T_{2g} phonon intensity, illustrating that increasing pressure suppresses the magnetic fluctuations and the magneto-optical response in CoCr_2O_4 by increasing the anisotropy field. Additionally, Fig. 8(b) shows that increasing pressure reduces the strong suppression of the T_{1g} -symmetry magnon intensity with increasing magnetic field in the Faraday geometry ($\mathbf{k} \parallel \mathbf{M} \parallel \mathbf{H}$), providing evidence that the magnetodielectric response of CoCr_2O_4 decreases with increasing pressure. Altogether, these results show that, by tuning magnetic anisotropy and reducing magnetic fluctuations of the Co^{2+} spins, pressure and epitaxial strain can be used as effective tuning parameters for controlling the magnetodielectric response of CoCr_2O_4 .

VI. SUMMARY AND CONCLUSIONS

In this paper, we showed that the $\mathbf{q} = 0$ T_{1g} -symmetry magnon in CoCr_2O_4 exhibits an anomalously large Raman scattering intensity, which reflects a large magneto-optical response that likely results from large magnetic fluctuations that couple strongly to the dielectric re-

sponse. The strong suppression of the T_{1g} -symmetry magnon Raman intensity in an applied field is consistent with the magnetodielectric response observed previously in this material,^{17,43} and suggests that the strong magnetodielectric response in CoCr_2O_4 results from the magnetic-field-induced suppression of magnetic fluctuations that are strongly coupled to phonons.¹⁶ Using pressure to increase the magnetic anisotropy in CoCr_2O_4 , we found that we can suppress the magnetic field-dependence of the T_{1g} -symmetry magnon Raman intensity by suppressing magnetic fluctuations, demonstrating that pressure or epitaxial strain should be an effective means of controlling magnetodielectric behavior and the magneto-optical response in CoCr_2O_4 . This Raman study also reveals conditions that are conducive for the substantial magneto-optical responses and magneto-

dielectric behaviors in materials, including the presence of strong spin-orbit coupling and weak magnetic anisotropy, both of which create favorable conditions for large magnetic fluctuations that strongly modulate the dielectric response.

ACKNOWLEDGMENTS

Research was supported by the National Science Foundation under Grant NSF DMR 1464090. RDM and DPS thank the Illinois Department of Materials Science and Engineering for support. X-ray diffraction and magnetic susceptibility measurements were performed in the Frederick Seitz Materials Research Laboratory.

-
- * asethi8@illinois.edu
 † slcooper@illinois.edu
- ¹ T. Kimura, T. Goto, H. Shintani, K. Ishizaka, T. Arima, and Y. Tokura, *Nature* **55**, 426 (2003), URL <http://www.nature.com/nature/journal/v426/n6962/full/nature02018.html>.
 - ² S.-W. Cheong and M. Mostovoy, *Nat. Mat.* **6**, 13 (2007).
 - ³ V. G. Bar'yakhtar and I. E. Chupis, *Sov. Phys. Solid State* **11**, 2628 (1970).
 - ⁴ A. Pimenov, A. A. Mukhin, V. Y. Ivanov, V. D. Travkin, A. M. Balbashov, and A. Loidl, *Nature Phys.* **2**, 97 (2006).
 - ⁵ N. Kida, Y. Ikebe, Y. Takahashi, J. P. He, Y. Kaneko, Y. Yamasaki, R. Shimano, T. Arima, N. Nagaosa, and Y. Tokura, *Phys. Rev. B* **78**, 104414 (2008), URL <http://link.aps.org/doi/10.1103/PhysRevB.78.104414>.
 - ⁶ N. Kida, Y. Yamasaki, R. Shimano, T. hisa Arima, and Y. Tokura, *Journal of the Physical Society of Japan* **77**, 123704 (2008), <http://dx.doi.org/10.1143/JPSJ.77.123704>, URL <http://dx.doi.org/10.1143/JPSJ.77.123704>.
 - ⁷ A. B. Sushkov, M. Mostovoy, R. V. Aguilar, S.-W. Cheong, and H. D. Drew, *Journal of Physics: Condensed Matter* **20**, 434210 (2008), URL <http://stacks.iop.org/0953-8984/20/i=43/a=434210>.
 - ⁸ R. Valdés Aguilar, M. Mostovoy, A. B. Sushkov, C. L. Zhang, Y. J. Choi, S.-W. Cheong, and H. D. Drew, *Phys. Rev. Lett.* **102**, 047203 (2009), URL <http://link.aps.org/doi/10.1103/PhysRevLett.102.047203>.
 - ⁹ M. P. V. Stenberg and R. de Sousa, *Phys. Rev. B* **80**, 094419 (2009), URL <http://link.aps.org/doi/10.1103/PhysRevB.80.094419>.
 - ¹⁰ M. Mochizuki, N. Furukawa, and N. Nagaosa, *Phys. Rev. Lett.* **104**, 177206 (2010), URL <http://link.aps.org/doi/10.1103/PhysRevLett.104.177206>.
 - ¹¹ S. Tiwari and D. Sa, *Journal of Physics: Condensed Matter* **22**, 225903 (2010), URL <http://stacks.iop.org/0953-8984/22/i=22/a=225903>.
 - ¹² A. B. Harris, arXiv:1011.6672v2 [cond-mat.mtrl-sci] (2011), URL <https://arxiv.org/pdf/1011.6672.pdf>.
 - ¹³ S. P. P. Jones, S. M. Gaw, K. I. Doig, D. Prabhakaran, E. M. H. Wheeler, A. T. Boothroyd, and J. Lloyd-Hughes, *Nature Communications* **5**, 3787 (2014).
 - ¹⁴ K. Cao, F. Giustino, and P. G. Radaelli, *Phys. Rev. Lett.* **114**, 197201 (2015), URL <http://link.aps.org/doi/10.1103/PhysRevLett.114.197201>.
 - ¹⁵ T. Kimura, S. Kawamoto, I. Yamada, M. Azuma, M. Takano, and Y. Tokura, *Phys. Rev. B* **67**, 180401 (2003), URL <http://link.aps.org/doi/10.1103/PhysRevB.67.180401>.
 - ¹⁶ G. Lawes, A. P. Ramirez, C. M. Varma, and M. A. Subramanian, *Phys. Rev. Lett.* **91**, 257208 (2003), URL <http://link.aps.org/doi/10.1103/PhysRevLett.91.257208>.
 - ¹⁷ S. Yang, H. X. Bao, D. Z. Xue, C. Zhou, J. H. Gao, Y. Wang, J. Q. Wang, X. P. Song, Z. B. Sun, X. B. Ren, et al., *Journal of Physics D: Applied Physics* **45**, 265001 (2012), URL <http://stacks.iop.org/0022-3727/45/i=26/a=265001>.
 - ¹⁸ T. Goto, T. Kimura, G. Lawes, A. P. Ramirez, and Y. Tokura, *Phys. Rev. Lett.* **92**, 257201 (2004), URL <http://link.aps.org/doi/10.1103/PhysRevLett.92.257201>.
 - ¹⁹ S. Bordács, D. Varjas, I. Kézsmárki, G. Mihály, L. Baldassarre, A. Abouelsayed, C. A. Kuntscher, K. Ohgushi, and Y. Tokura, *Phys. Rev. Lett.* **103**, 077205 (2009), URL <http://link.aps.org/doi/10.1103/PhysRevLett.103.077205>.
 - ²⁰ K. Singh, A. Maignan, C. Simon, and C. Martin, *Applied Physics Letters* **99**, 172903 (2011), URL <http://scitation.aip.org/content/aip/journal/apl/99/17/10.1063/1.3656711>.
 - ²¹ K. Tomiyasu, J. Fukunaga, and H. Suzuki, *Phys. Rev. B* **70**, 214434 (2004), URL <http://link.aps.org/doi/10.1103/PhysRevB.70.214434>.
 - ²² V. Tsurkan, S. Zherlitsyn, S. Yasin, V. Felea, Y. Skourski, J. Deisenhofer, H.-A. K. von Nidda, J. Wosnitza, and A. Loidl, *Phys. Rev. Lett.* **110**, 115502 (2013), URL <http://link.aps.org/doi/10.1103/PhysRevLett.110.115502>.
 - ²³ Y. Yamasaki, S. Miyasaka, Y. Kaneko, J.-P. He, T. Arima, and Y. Tokura, *Phys. Rev. Lett.* **96**, 207204 (2006), URL <http://link.aps.org/doi/10.1103/PhysRevLett.96.207204>.
 - ²⁴ G. Lawes, B. Melot, K. Page, C. Ederer, M. A. Hayward, T. Proffen, and R. Seshadri, *Phys. Rev. B* **74**, 024413 (2006), URL <http://link.aps.org/doi/10.1103/PhysRevB.74.024413>.

- ²⁵ Y. J. Choi, J. Okamoto, D. J. Huang, K. S. Chao, H. J. Lin, C. T. Chen, M. van Veenendaal, T. A. Kaplan, and S.-W. Cheong, Phys. Rev. Lett. **102**, 067601 (2009), URL <http://link.aps.org/doi/10.1103/PhysRevLett.102.067601>.
- ²⁶ H. Katsura, N. Nagaosa, and A. V. Balatsky, Phys. Rev. Lett. **95**, 057205 (2005), URL <http://link.aps.org/doi/10.1103/PhysRevLett.95.057205>.
- ²⁷ M. Mostovoy, Phys. Rev. Lett. **96**, 067601 (2006), URL <http://link.aps.org/doi/10.1103/PhysRevLett.96.067601>.
- ²⁸ V. I. Torgashev, A. S. Prokhorov, G. A. Komandin, E. S. Zhukova, V. B. Anzin, V. M. Talanov, L. M. Rabkin, A. A. Bush, M. Dressel, and B. P. Gorshunov, Physics of the Solid State **54**, 350 (2012), ISSN 1090-6460, URL <http://dx.doi.org/10.1134/S1063783412020321>.
- ²⁹ D. Kamenskyi, H. Engelkamp, T. Fischer, M. Uhlarz, J. Wosnitzer, B. P. Gorshunov, G. A. Komandin, A. S. Prokhorov, M. Dressel, A. A. Bush, et al., Phys. Rev. B **87**, 134423 (2013), URL <http://link.aps.org/doi/10.1103/PhysRevB.87.134423>.
- ³⁰ A. K. Kushwaha, Chinese Journal of Physics **47**, 355 (2009), ISSN 0577-9073.
- ³¹ M. Ptak, M. Mczka, A. Pikul, P. Tomaszewski, and J. Hanuza, Journal of Solid State Chemistry **212**, 218 (2014), ISSN 0022-4596, URL <http://www.sciencedirect.com/science/article/pii/S0022459613005264>.
- ³² I. Efthimiopoulos, Z. T. Y. Liu, S. V. Khare, P. Sarin, T. Lochbiler, V. Tsurkan, A. Loidl, D. Popov, and Y. Wang, Phys. Rev. B **92**, 064108 (2015), URL <http://link.aps.org/doi/10.1103/PhysRevB.92.064108>.
- ³³ T. Kanomata, T. Tsuda, H. Yasui, and T. Kaneko, Physics Letters A **134**, 196 (1988), ISSN 0375-9601, URL <http://www.sciencedirect.com/science/article/pii/0375960188908201>.
- ³⁴ S. Tamura, Physica B: Condensed Matter **190**, 150 (1993), ISSN 0921-4526, URL <http://www.sciencedirect.com/science/article/pii/092145269390460N>.
- ³⁵ X. Chen, Z. Yang, Y. Xie, Z. Huang, L. Ling, S. Zhang, L. Pi, Y. Sun, and Y. Zhang, Journal of Applied Physics **113**, 17E129 (2013), URL <http://scitation.aip.org/content/aip/journal/jap/113/17/10.1063/1.4796172>.
- ³⁶ S. L. Gleason, T. Byrum, Y. Gim, A. Thaler, P. Abbamonte, G. J. MacDougall, L. W. Martin, H. D. Zhou, and S. L. Cooper, Phys. Rev. B **89**, 134402 (2014), URL <http://link.aps.org/doi/10.1103/PhysRevB.89.134402>.
- ³⁷ Y. Gim, A. Sethi, Q. Zhao, J. F. Mitchell, G. Cao, and S. L. Cooper, Phys. Rev. B **93**, 024405 (2016), URL <http://link.aps.org/doi/10.1103/PhysRevB.93.024405>.
- ³⁸ T. Byrum, S. L. Gleason, A. Thaler, G. J. MacDougall, and S. L. Cooper, Phys. Rev. B **93**, 184418 (2016), URL <http://link.aps.org/doi/10.1103/PhysRevB.93.184418>.
- ³⁹ M. Cazayous, Y. Gallais, A. Sacuto, R. de Sousa, D. Lebeugle, and D. Colson, Phys. Rev. Lett. **101**, 037601 (2008), URL <http://link.aps.org/doi/10.1103/PhysRevLett.101.037601>.
- ⁴⁰ M. K. Singh, R. S. Katiyar, and J. F. Scott, Journal of Physics: Condensed Matter **20**, 252203 (2008), URL <http://stacks.iop.org/0953-8984/20/i=25/a=252203>.
- ⁴¹ P. Rovillain, M. Cazayous, Y. Gallais, A. Sacuto, M.-A. Measson, and H. Sakata, Phys. Rev. B **81**, 054428 (2010), URL <http://link.aps.org/doi/10.1103/PhysRevB.81.054428>.
- ⁴² P. Rovillain, M. Cazayous, Y. Gallais, M.-A. Measson, A. Sacuto, H. Sakata, and M. Mochizuki, Phys. Rev. Lett. **107**, 027202 (2011), URL <http://link.aps.org/doi/10.1103/PhysRevLett.107.027202>.
- ⁴³ N. Mufti, A. A. Nugroho, G. R. Blake, and T. T. M. Palstra, Journal of Physics: Condensed Matter **22**, 075902 (2010), URL <http://stacks.iop.org/0953-8984/22/i=7/a=075902>.
- ⁴⁴ K. Ohgushi, Y. Okimoto, T. Ogasawara, S. Miyasaka, and Y. Tokura, Journal of the Physical Society of Japan **77**, 034713 (2008), <http://dx.doi.org/10.1143/JPSJ.77.034713>, URL <http://dx.doi.org/10.1143/JPSJ.77.034713>.
- ⁴⁵ J. Bézar and G. Baldinozzi, IUCr-CPD Newsletter **20**, 3 (1998).
- ⁴⁶ M. Kim, X. M. Chen, X. Wang, C. S. Nelson, R. Budakian, P. Abbamonte, and S. L. Cooper, Phys. Rev. B **84**, 174424 (2011), URL <http://link.aps.org/doi/10.1103/PhysRevB.84.174424>.
- ⁴⁷ M. G. Cottam and D. J. Lockwood, *Light Scattering in Magnetic Solids* (Wiley-Interscience, New York, 1986).
- ⁴⁸ A. K. Ramdas and S. Rodriguez, Topics in Applied Physics **68**, 137 (1991).
- ⁴⁹ J. Kaplan and C. Kittel, J. Chem. Phys. **5**, 760 (1953), URL <http://scitation.aip.org/content/aip/journal/jcp/21/4/10.1063/1.1699018>.
- ⁵⁰ W. F. Brinkman and R. J. Elliott, Proceedings of the Royal Society of London, Series A: Mathematical, Physical and Engineering Sciences **294**, 343 (1966), ISSN 0080-4630, <http://rspa.royalsocietypublishing.org/content/294/1438/343.full.pdf>, URL <http://rspa.royalsocietypublishing.org/content/294/1438/343>.
- ⁵¹ V. Sahni and G. Venkataraman, Advances in Physics **23**, 547 (1974), <http://dx.doi.org/10.1080/00018737400101391>, URL <http://dx.doi.org/10.1080/00018737400101391>.
- ⁵² S. O. Demokritov, N. M. Kreines, and V. I. Kudinov, Sov. Phys. JETP **65**, 389 (1987).
- ⁵³ A. Kumar, J. F. Scott, and R. S. Katiyar, Applied Physics Letters **99**, 062504 (2011), URL <http://scitation.aip.org/content/aip/journal/apl/99/6/10.1063/1.3624845>.
- ⁵⁴ V. G. Bar'yakhtar, Y. G. Pashkevich, and V. L. Sobolev, Sov. Phys. JETP **58**, 945 (1983).
- ⁵⁵ A. S. Borovik-Romanov and N. M. Kreines, in *Spin Waves and Magnetic Excitations* (North-Holland, Amsterdam, 1988), chap. 2.
- ⁵⁶ I. Vitebskii, A. Yeremenko, Y. Pashkevich, V. Sobolev, and S. Fedorov, Physica C: Superconductivity **178**, 189 (1991), ISSN 0921-4534, URL <http://www.sciencedirect.com/science/article/pii/092145349190175X>.
- ⁵⁷ S. A. Altshuler and B. M. Kozyrev, *Electron Paramagnetic Resonance in Compounds of Transition Elements* (Wiley, New York, 1974).
- ⁵⁸ G. A. Smolenski and I. E. Chupis, Soviet Physics Uspekhi **25**, 475 (1982), URL <http://stacks.iop.org/0038-5670/25/i=7/a=R02>.